BIOCHEMICAL IMAGING OF HUMAN BRAIN GLIOMAS WITH SYNCHROTRON RADIATION MICROPROBE

M. Szczerbowska-Boruchowska[1], S. Wojcik[1], M. Kastyak[1], J. Chwiej[1], Z. Stegowski[1], M. Lankosz[1], D. Adamek[2]

[1]Faculty of Physics and Applied Computer Science, AGH, University of Science and Technology, Krakow, Poland;

[2]Institute of Neurology, Collegium Medicum, Jagiellonian University, Krakow, Poland

Introduction

The brain gliomas are the most common major histologic type of brain cancer and account for more than 40% of all neoplasms of central neurvous system [1]. A majority of gliomas are diffuse astrocytic tumors classified into three grades by the World Health Organization (WHO grade II, III, and IV tumors). In spite of the frequency of occurrence the knowledge of this type of cancer is still very poor. Moreover, in the last years the therapeutic progress with reference to gliomas is the least compared to the other neoplasms. The causes and pathogenesis of brain tumors are not well understood and current therapies are relatively ineffective [1]. The determination of elemental composition of the tumor tissue at the single cell level coupled with the analysis of sulfur oxidation states as well as determination of biomolecules is particularly essential considering biochemical processes that may participate in pathogenesis of the brain gliomas. As it is supposed some elements may participate carcinogenesis for example by oxidative damage (mainly Fe, Cu, Mn) [2,3] or by promotion of angiogenesis (Cu) [4]. From the other side selected elements such as Se, Zn, Cu elements play an important role in the protection of the organism against the mechanisms that can initiate or accelerate the carcinogenesis. Moreover, some elements may play a role in the potential neurotoxic influence of the tumor on the surrounding tissue by selected processes like oxidative stress (Fe, Cu, Zn, Mn) [5], excitotoxicity (Ca) [6], disfunction of metalo-dependent enzymes like Mn-SOD (Mn) or Cu/Zn-SOD (Cu, Zn) [7] and others. It is known that malignant cell proliferation may be related to a deficiency of sulfane sulfur and the uncontrolled operation of a set of enzymes normally inactivated by sulfane sulfur. Since biochemical changes may be related to the growth rate of cancer cells, they can be thought of as markers of tumor cell proliferation [8]. A confirmation of the increased level of reduced sulfur atoms (-2 and 0 valence) in malignant gliomas is of great importance.

The diagnosis and grading of individual gliomas is based primarily on morphological pattern recognition (assessed by the microscope examination of hematoxylin-eozine-stained tissue sections). Immunohistochemical markers and molecular approaches have also been integrated into the classification of gliomas with respect to their glial lineage (e.g., whether astrocytic or oligodendroglial), their clinical behavior, and their response to treatment [9]. However, the routine use of molecular genetic-related markers is laborious, requires suitable technical means, and is thus time- and money-consuming. Furthermore, the high level of heterogeneity frequently encountered in gliomas (at histological, biological and molecular levels) does not facilitate the use of such markers [10]. Significant attention has recently focused on molecular approaches with the aim of improving tumor classification and the resultant stratification of patients for prognosis and treatment purposes. Diagnostic methods based on FTIR spectroscopy emerged and developed rapidly during the last decade. This technique could usefully complement information provided by more conventional diagnostic and prognostic approaches with respect to brain gliomas.

Sample preparation

Tissue specimens were taken intraoperatively from patients with different grades of brain gliomas. These samples were taken from two areas i.e. tumor center and extratumoral tissue without malignant infiltration (confirmed histopathologically).The specimens were frozen and cut into sections of 20 or 10 micrometers thick in a cryo-microtome. The slices were fixed onto ultralene foil and freeze dried at -20 °C.

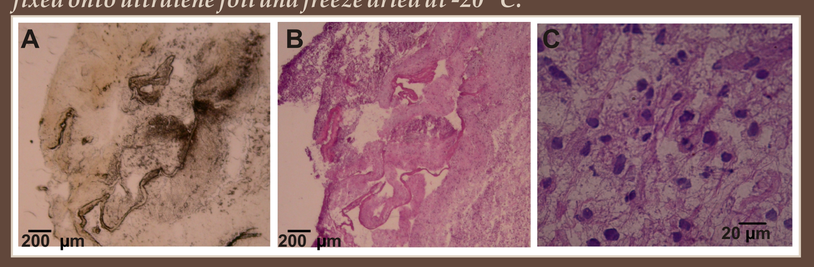

Fig. 1. Microscopic view of human brain glioma (oligodendroglioma - WHO II) sections. A)Tissue slice dedicated to spectroscopic analyses; B)&C) hematoxylin-eosin stained sections.

Synchrotron Radiation X-Ray Fluorescence (SR-XRF) Imaging

The SR-XRF measurements were performed at the bending magnet beamline L at HASYLAB. The primary photon energy was set to 17 keV. To reduce the beam size the high flux capillary was used. The beam was focused to a size of 15 µm in diameter. Two-dimensional maps of selected element distribution were determined. The step sizes applied for mapping were equal to 15 µm both horizontally and vertically. The time of acquisition was equal to 10 s per pixel. The measurements were carried out in air. The characteristic X-ray lines were measured by the Vortex SDD detector from SII Nano Technology USA Inc. The measurements of either NIST standard reference materials (SRM 1833 and SRM 1832) or thin film XRF calibration standards were performed for the determination of masses per unit area of elements.

The preliminary research showed that for all cases the elements such as P, S, Cl, K, Ca, Fe, Cu, Zn, Br and Rb were present in human brain glioma cells. Additionally, in selected samples the elements such as Hg, La, Ni, Ru and Gd (result of applying of Gd-containing magnetic resonance imaging agent) were detected. A typical sum spectrum excited inside brain glioma cell is presented in Fig. 2. Two dimensional maps of elemental distribution in the tumor were obtained. The selected results were presented in Fig. 3.

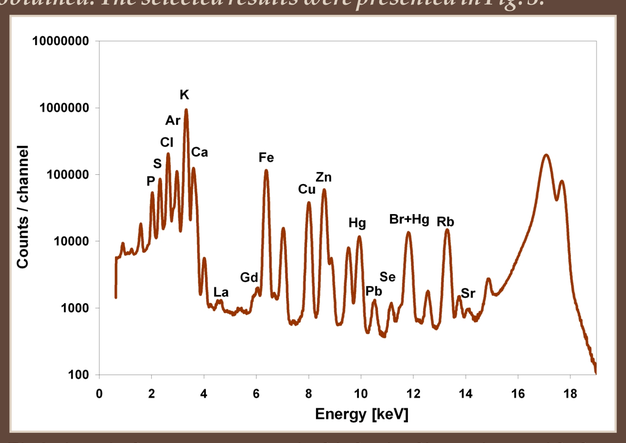

Fig.2. A typical sum spectrum excited in brain glioma tissue with the use of synchrotron radiation (beam energy 17 keV).

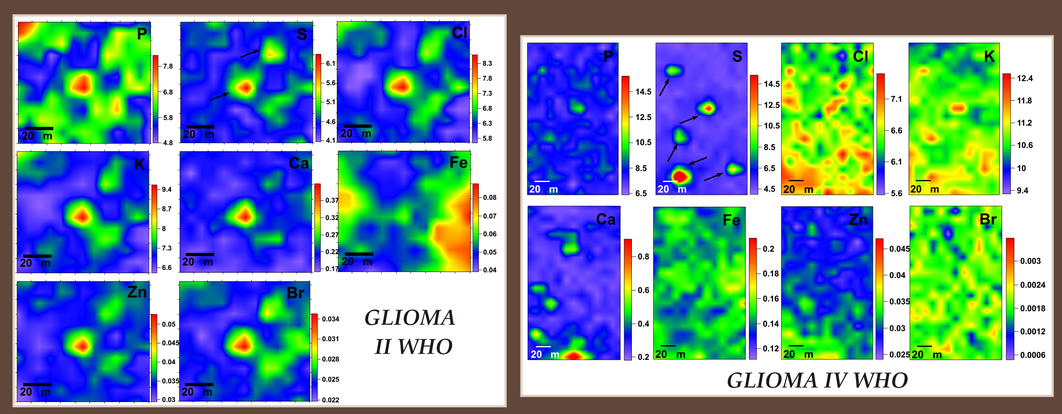

Fig. 3. Distribution of selected elements in human brain glioma tissue for II (left) and IV (right) grade malignancy. The arrows show cancer cells. Data presented in µg/cm^2.

X-Ray Absorption Near Eadge Structure Spectroscopy (XANES)

The experiment was carried out on the undulator beamline ID21 at ESRF. X-ray absorption near edge structure (XANES) spectroscopy at the sulfur K-edge was applied using the scanning X-ray microscope in fluorescence mode. The microscope used a Fresnel zone-plate as a focusing lens and delivered a microbeam of 0.5 x 0.5 µm^2. The thin tissue sections of human brain gliomas with different grades of glioma malignancy as well as tissue without malignant infiltration were probed. As the reference materials the following organic compounds were applied: glutathione (oxidized and reduced form), cysteine, cystine, methionine, dimethyl sulphoxide, cysteic acid, zinc sulphate, sodium tetrathionate, sodium thiosulfate.

For selected points of the tissue section the structure of S K absorption edge was studied. Micro-XANES spectra at the sulfur K-edge collected inside cancer cell, its boundary and surrounding tissue in comparison with the spectra obtained for zinc sulfate and methionine were presented in Fig. 4. Oxidation states imaging involved scanning a sample in two dimensions with spatial resolution equal to 0.5 µm on each direction. Typical area of scanning was 100 x 100 µm^2. The step size was equal to the incident photons beam i.e. 0.5 µm. The monochromator was set to the appropriate energy for the edge of S oxidation states. Mapping of the different forms of sulfur was performed at energies of 2.4735 keV (S^{2-}), 2.4764 keV (S^{4+}), 2.4825 keV (S^{6+}) and 2.5000 keV (total S). The results obtained for cancerous tissue (II and IV stage of glioma malignancy) and control sample were illustrated in Fig. 5. As it is shown cancer cells accumulate sulfur mainly as sulfide (S^{2-}) form. The preliminary results indicated also higher accumulation of this form of sulfur in glioma of IV grade of malignancy in comparison with the samples of II grade neoplasms. The presence of sulfate (S^{+6}) species was revealed in histological structures outside the cancer cells. The sulfite (S^{+4}) form of sulfur was not detected in the cancer cells.

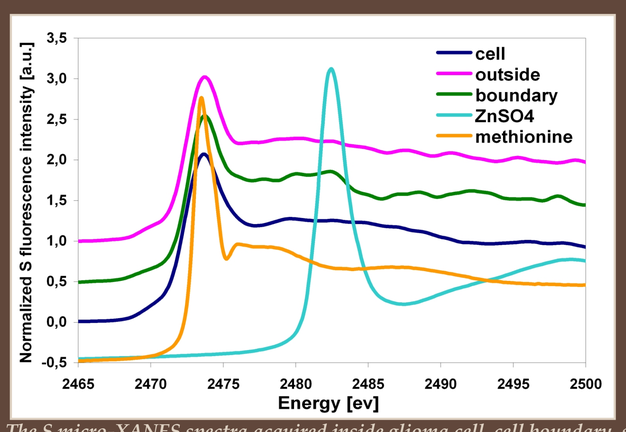

Fig. 4. The S micro-XANES spectra acquired inside glioma cell, cell boundary, surrounding tissue, methionine and zinc sulfate.

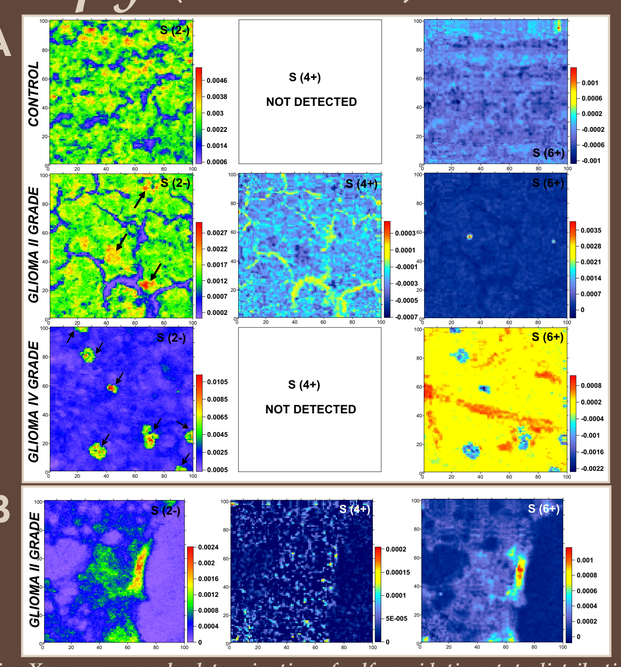

Fig. 5. Scanning X-ray mocroprobe determination of sulfur oxidation state distribution in A) brain glioma and control samples; B) glioma tissue area without cancer cells (area: 100 x100 µm^2). The arrows in A) show cancer cells. Data presented in arbitrary units.

Synchrotron Radiation Fourier Transform Infrared Microspectroscopy (SR-FTIR)

The FTIR measurements were carried out on ID21 infrared endstation at ESRF. The IR microspectroscopic maps were collected in transmission mode using a Infrared microscope coupled to a FTIR spectrometer. Most of the analysis and maps presented were achieved with a projected area on the sample, of 8 x 8 µm^2 and a step size of 6 µm, and each spectra were acquired after 100 accumulations at 8 cm^{-1} spectral resolution. Data acquisition and processing were performed using Omnic software (Version 7.0, Thermo-Nicolet).

A comparison of the IR absorption spectra collected inside cancer cell and tissue area without malignant infiltration was illustrated in Fig. 6. The major spectral differences between control and cancerous tissues were identified at the following vibrational frequencies: 3300 cm^{-1}, 2925 cm^{-1}, 2830 cm^{-1}, 1655 cm^{-1},1545 cm^{-1} and 1086 cm^{-1}. The tissue areas were mapped to generate two-dimensional images of the main biological molecules of interest. Integrated intensities of selected bands were extracted after raster scanning of the sample. The infrared maps of the selected functional groups enabled to find precise distribution of biomolecules in cancer cells that was presented in Fig. 7.

Table 1. Tentative assignments of the bands frequencies indicated in Fig. 6.

Frequency [cm^{-1}]	Assignment	Frequency [cm^{-1}]	Assignment
3400-3200	OH str	~1545	Amide II: NH bend vib, CN str (protein)
~3300	N-H str (protein, amide A)	~1460	CH_2 sciss vib; CH_3 asym bend vib (lipids)
~3080	N-H str (protein, amide B)	~1380	CH_3 sym bend vib (lipids)
~2930	CH_2 asym str (lipids)	~1300	Amide III: CN str, NH bend,CO str, O=C-N bend vib
~2850	CH_2 sym str (lipids)	1260-1220	PO_2 asym str (nucleic aids)
1750-1720	C=O str (ester, lipids)	~1170	CO-O-C asymmetric stretching (lipid)
~1655	Amide I: CO str, CN str, NH bend vib	~1085	PO_2 sym str (nucleic aids)

str stretching; asym asymmetric; sym symmetric; bend bending; vib vibration; sciss - scissoring

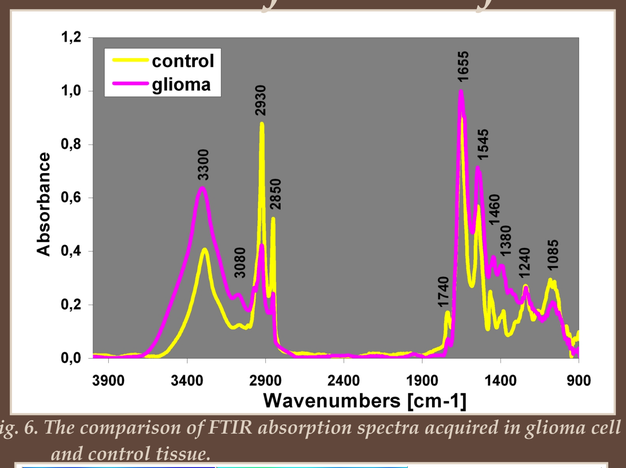

Fig. 6. The comparison of FTIR absorption spectra acquired in glioma cell and control tissue.

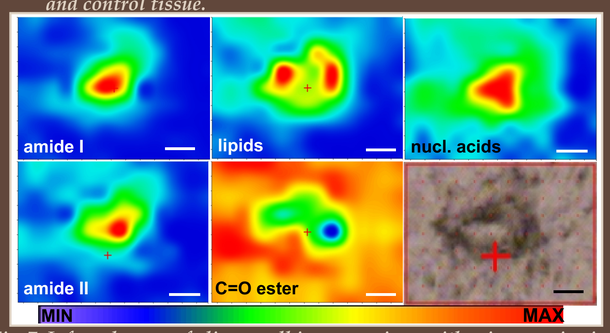

Fig. 7. Infrared maps of glioma cell in comparison with microscopic view of scanned area of the tissue. Scale bar: 10 µm.

References

1. R. Lewis. The Role of Ageing in Glioma Pathogenesis. Http://detserv1.dl.ac.uk/Herald/ageing&glioma.html
2. Goldhaber SB. Regulatory Toxicology and Pharmacology. 2003; 38:232
3. Toyokuni S. Free Radical Biology and Medicine, 1996; 20(4): 553
4. Hu GF. J Cell Biochem. 1998; 69:326
5. Bains JS, Shaw CA. Bain Res. Rev. 1997; 25: 335
6. Morrison BM, Morrison JH. Brain Res. Rev. 1999; 29: 121
7. Bush AI. Current Opinion in Chemical Biology. 2000; 4: 184
8. Wrobel M., Czubak J., Adamek D., Bronowicka P., Czepko R. Folia Neuropatologica 2005; 43/3:224
9. P. Kleihues, W.K. Cavenee, Pathology and genetics of tumours of the nervous system. in: International Agency for Research on Cancer (IARC) WHO health Organisation (Ed.), Oxford Press, Oxford, 2000.
10. Camby, I Salmon, A Danguy, J.L Pasteels, J Brotchi, J Martinez, R Kiss, Influence of gastrin on human astrocytic tumor cell proliferation, J. Natl. Cancer Inst. 1996; 88: 594

Acknowledgements

The authors acknowledge the European Synchrotron Radiation Facility and the Hamburger Synchrotronstrahlungslabor HASYLAB at Deutsches Elektronen-Synchrotron DESY for provision of synchrotron radiation facilities. The authors would like to thank Dr Jean Susini (ESRF), Dr M. Cotte (ESRF), Dr G. Falkenberg (HASYLAB) and Dr Karen Rickers-Appelt (HASYLAB) for assistance in using beamlines ID21 (ESRF), ID22 (ESRF) and beamline L (HASYLAB). This work was supported by the Ministry of Science and High Education (Warsaw, Poland) and the following grants: DESY/304/2006 (2007-2009; Ministry of Science and High Education, Warsaw, Poland); 155/ESR/2006/03 (Ministry of Science and High Education, Warsaw, Poland); The European Community-Research Infrastructure Action under FP6 "Structuring the European Research Area" Programme (through the Integrated Infrastructure Initiative "Integrating Activity on Synchrotron and Free Electron Laser Science"); Contract RII3-CT-2004-506008 (IA-SFS).